33RD CONGRESS
OF THE INTERNATIONAL COUNCIL
OF THE AERONAUTICAL SCIENCES
STOCKHOLM, SWEDEN, 4-9 SEPTEMBER, 2022

ICAS 2022 SWEDEN

WIND TUNNEL EXPERIMENT WITH AN EPP-WING TO INVESTIGATE AEROELASTIC EFFECTS OF NONLINEAR ELASTIC STIFFNESSES

Kjell Bramsiepe[1], Marc Braune[1], Wolf Krüger[1] & Lorenz Tichy[1]

[1]DLR - German Aerospace Center, Institute of Aeroelasticity, kjell.bramsiepe@dlr.de

Abstract

Background: Nonlinear elastic, especially degressive, stiffnesses can reduce the wing root bending moment for design loadcases, while the cruise flight shape remains unchanged.
Objective: The aim of the wind tunnel experiment is to show up the behaviour of a wing with a degressive stiffness. The tested wing is made of expanded polypropylene foam (EPP).
Method: A flexural bending test is conducted to gain the bending stiffness of EPP for different densities and a wind tunnel test is performed to obtain the dependency between bending moment and deflection. The findings are compared to the results of an aeroelastic method based on a nonlinear elastic beam.
Results: The bending stiffness of EPP material exhibit a nonlinear degressive stiffness. The foam wing has a softening characteristic for ascending loads. The numerical beam method for nonlinear elastic wings shows up a good agreement with the experiment and points out the load reducing effect of nonlinear structures.

Keywords: hyperelastic stiffness, aeroelasticity, validation experiment, foam wing, load alleviation

1. Introduction

Wings of aircraft should become lighter and more efficient to save fuel consumption and costs. Wing structures behave almost linearly. Thus, doubling the loads leads to a doubling of the wing deflection. At the same time, the bending torsion coupling of swept wings influences the load distribution. Higher deflections at the wing tip result in lower incidence angles at the wing tip, which is followed by a reduction of the root bending moment. In the research field of aeroelastic tailoring, the layup of fibre reinforced laminates is optimised to influences this coupling beneficially [1, 2].
The constitutive idea is to modify the linear properties of wing structures to influence the deflection and lift distribution with the effects of the bending torsion coupling. With such a nonlinear structure technology, the advantageous deflection for intense loading conditions are enlarged while the change of the wing deformation around the design point is minimised to improve the aerodynamic performance at 'off'-conditions. This idea is comparable to a palm tree which bends in stormy weather and stands straight during sunny conditions.
The semi aeroelastic hinged wing concept (AlbatrossOne) utilises a hinged wing tip device to change the stiffness at that position [3]. In doing so, the moment force of the wing tip can be neutralised at the hinge position and the root bending moment is reduced. This nonlinear stiffness concept is an active load alleviation concept which can be switched between two states (fixed and free wing tip). In addition, the concept is located at one fixed position of the hinge. Our concept aims for a passive solution which acts along the whole wing span.
Hyperelastic effects are known by shape memory alloys, e.g. NiTi-alloy [4]. Its stress strain relation has a high initial stiffness followed by a stiffness plateau where the strains increase and the stresses stay almost constant. After a certain strain value the stiffness regains. This effect results from a change in the crystal structure of such an alloy. The disadvantage for wing structures is the temperature dependence of this effect. Foam materials, like expanded polypropylene (EPP), are highly flexible as well and also exhibit nonlinear elastic stiffnesses [5]. To test these foam materials, small

wind tunnel models out of EPP are useful. For real wing structures, aluminum foams may be used to create nonlinear stiffness effects. Sandwich structures with aluminum foam were tested by Yao et al. [6] with regard to their fatigue behaviour. Buckling of plates can also lead to a stiffness reduction which can be utilised to reduce the stiffness of a wing structure.
In the research field of EPP, Weingart et al. [7] tested EPP with a density of 10 g/l and compared it to an expanded polycarbonate foam (EPC) which is less temperature dependent. A lot of tests are performed to analyse the compression properties of foam material; a few have tested also the tension properties. However, in this investigation we will focus on the combined stiffness of EPP-foam material in a bending test, and this for four types of density.
In our recent work, a nonlinear beam method with aeroelastic coupling was developed to analyse the aeroelastic interactions of such technologies. Furthermore, a reduction of the root bending moment was shown for a degressive stiffness behaviour [8, 9]. Hence, the goal of this paper is to demonstrate the aeroelastic possibilities of nonlinear elastic behaviours with a foam material wing in a wind tunnel test campaign.

2. Experimental Test Setup

2.1 Three-Point Flexural Bending Test Setup

For the investigation of the material properties of EPP a simple flexural test rack was built (Fig. 1 d). Four material densities were tested with the beam dimensions of 400mm x 50mm x 10mm (L x a x b). The used densities were 30 g/l, 60 g/l, 100 g/l and 150 g/l. The probes were cut out of a 400mm square plate with a heated knife. The loading of the probe was conducted with a set of weights (m) attached to the center between the two supports. The supports had a distance l of 350 mm. The force F and reaction forces were calculated statically. The deflection Δz was measured by a laser distance measurements on top of the load bracket.

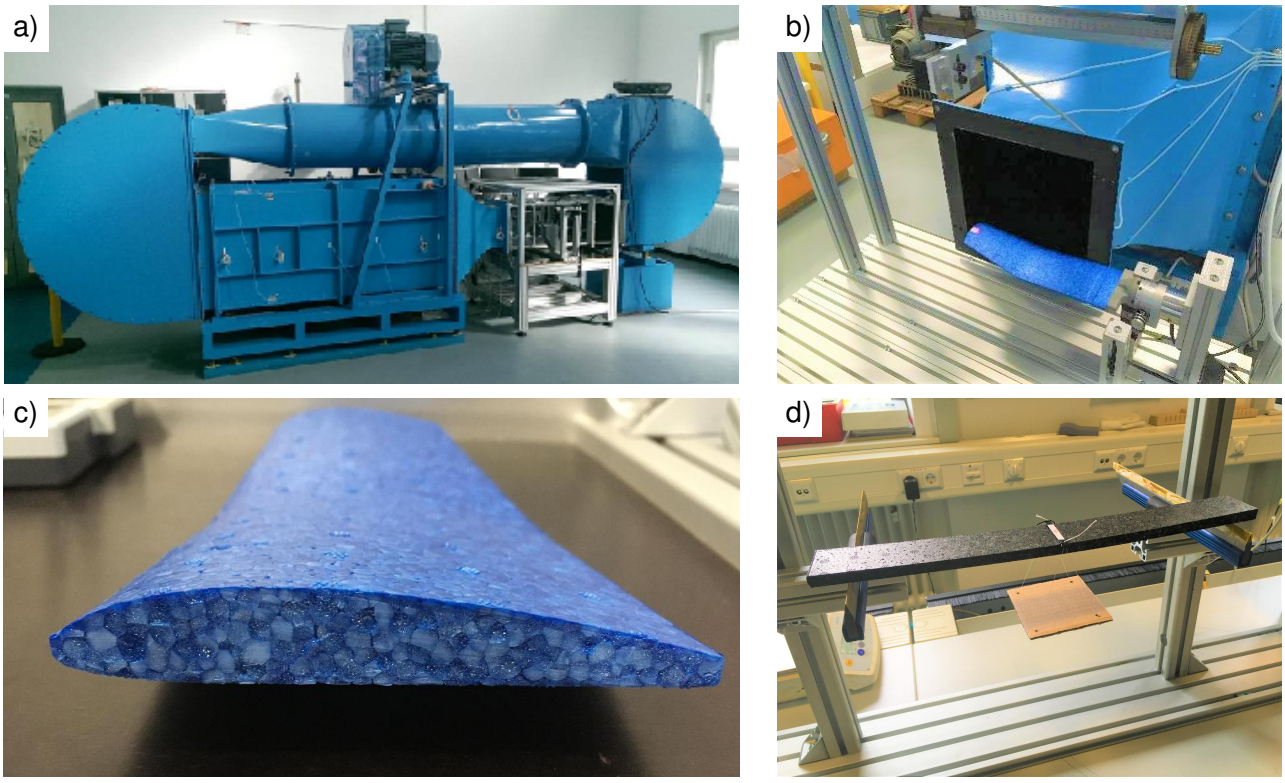

Figure 1 – Test setup - a) wind tunnel b) Top-back view c) cross section d) three-point bending test

The maximum bending moment M_{max}, in the middle of the probe, depends on the loading force and the support distance.

$$M_{max} = \frac{F \cdot l}{4} \tag{1}$$

The maximum strain ε_{max} is located at the bottom of the probe.

$$\varepsilon_{max} = \frac{\Delta z \cdot b/2 \cdot 12}{l^2} \tag{2}$$

The maximum stress can be calculated for every measuring point with:

$$\sigma_{max} = \frac{M_{max}}{I} \cdot \frac{b}{2} \tag{3}$$

Then, for each step, the E modulus can be obtained by:

$$E_i = \frac{\sigma_{i+1} - \sigma i}{\varepsilon_{i+1} - \varepsilon i} \tag{4}$$

So, a multi-linear formulation describes the material characteristics. The beams were loaded cyclically (1 min loading, 5 min recovery). During the last 10 seconds of each phase, loaded and unloaded, the deflection of the beam was recorded. To reduce the thermal influences, the temperature was controlled.

2.2 Wind Tunnel Test Setup

The test, presented here, was conducted in the Göttingen type wind tunnel of the DLR - Institute of Aeroelasticity (Fig. 1 a) with a subsonic velocity range up to 50 m/s. Input parameters were the velocity, the angle of attack, and the sweep angle of the wing. Besides the input parameters, the deformation of the wing was measured by laser distance measurement at two spanwise positions (L1 $\hat{=}$ wingtip / L2 $\hat{=}$ half wing span).

The wing structure consists of EPP and is foamed up in the wing mould by Miniprop. The density of the wing is 30 g/l. It has a half-span of 30 cm with a root chord of 10 cm and a tip chord of 7 cm. The outer half of the wing has a dihedral shape. The wing structure was supported by a 3D-printed clamp at the root. So, the wing can be represented by a cantilever beam in the numerical analysis. A set of different angles of attack and sweep angles was conducted to show up the nonlinear elastic behaviour and its influence on the sectional forces at the root. In Figure 1 both test setups are shown.

The angle of attack was measured by two laser triangulators at the root. The global aerodynamic forces were measured with a 6-component strain gauge balance at the clamp. The position of the laser system for measuring the deflection curve was changed in x and y directions, to measure the pure Δz deflection. The wind tunnel velocity had been calibrated with a pressure probe at the leading edge position before the wing was installed.

The wing was also loaded cyclically (1 min loading, 5 min recovery). Again, the last 10 second of each period were measured. In doing so, the creeping deflection is kept to an equal offset and can be neglected.

3. Numerical Analysis

The numerical method is based on the classical beam method. Hooke's law is replaced by a stepwise formulation of the stiffness relation between stress and strain. By integrating the stress of the cross section, a relation between the bending moment and curvature can be evolved. This relation is used inside the formulation of a beam element. The deflection of the wing structure is calculated with 30 beam elements in a finite element analysis. With this method, any multi-linear stiffness relation can be inserted. The curvature κ is dependent on the constant bending moment $M_{b,y}$ for a beam element with the following equations which are valid for the intermediate linear steps of the material:

$$\kappa(M_{b,y}) = \frac{1}{6B_i}\left(\frac{K_i^2 + L_i^{\frac{2}{3}}}{L_i^{\frac{1}{3}}} + K_i\right) \tag{5}$$

The simplification factors K and L are defined by:

$$K_i = 2 \cdot \left(\frac{M_{b,y}}{I_y} - A_i\right), \qquad L_i = K_i^3 - 108C_iB_i^2 + 6B_i\sqrt{3C_i(-2K_i^3 + 108C_iB_i^2)} \tag{6}$$

The stiffness properties of the material is extended with the material values A, B and C, while B is equal to the E-modulus of the intermediate step.

$$A_n = -\frac{3}{2} \cdot \sum_{i=1}^{n} (E_i - E_{i-1}) \cdot \kappa_{i-1}, \qquad B_n = E_n, \qquad C_n = \frac{1}{2} \cdot \sum_{i=1}^{n} (E_i - E_{i-1}) \cdot \kappa_{i-1}^3 \tag{7}$$

The curvature end points κ_i, from which the next step of the material begins to act, are also fixed material values which depends on the strain end points ε_i and the thickness of the beam b.

$$\kappa_i = \frac{\varepsilon_i}{b/2} \tag{8}$$

The values ε_i, σ_i and E_i are defined by the multi-linear material data for each step (see Fig. 2). The aerodynamic loads are calculated with the vortex lattice method. The quasi-steady solution is calculated in an iterative loop of structural analysis and load analysis. The aerodynamic forces are coupled with the beam by rigid elements with the shortest distances between every panel node and the structural grid. Geometric nonlinear effects are not considered to show up the pure potential of the stiffness nonlinearity. In doing so, the results are reasonable up to a deformation of 15% of the wing half-span. Nevertheless, the results with higher deformations show the tendency of the predefined structural behaviour. More details of the method and the derivation can be found in our recent work [9].

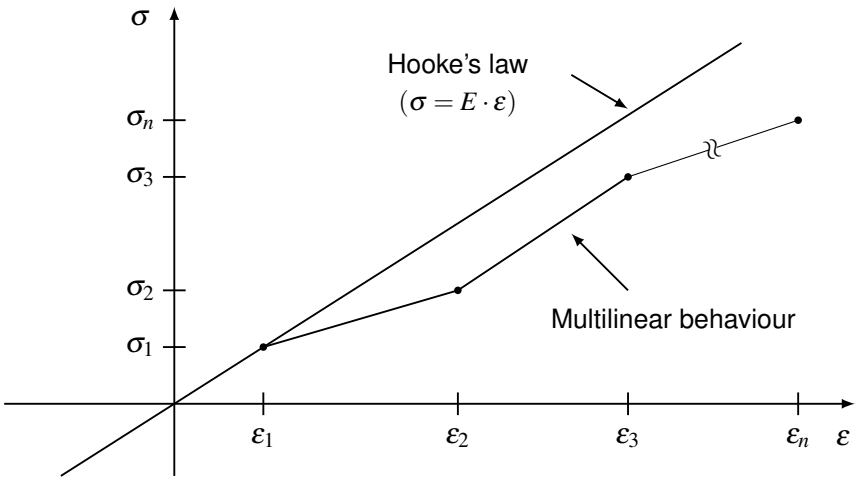

Figure 2 – Hooke's law and definition of end points for the nonlinear elastic stiffness

4. Experimental Results

4.1 Results of the flexural test

The deflections of the beam in dependency on the given loading and their stress and strain results are shown in Figure 3. Obviously, the deflections increase progressively with increasing loading. For higher densities, the initial stiffness of the material is higher. However, the nonlinear characteristics are more prevalent. The plastic deformation (dotted lines), after 5 min of recovery time, is relatively low in comparison to the elastic deformation component.

The E-moduli in Figure 4 are calculated for each step. They show up a strong variation in the measurements of the higher densities. They can be explained by the abrasive edges of the probe which cause small jerks. A visible example for this can be seen at Δz = 30 mm of the 100 g/l-curve. Hence, the E-modulus was calculated for bigger areas with a step-size of 0.005 m/m on the strains. These are given as trend lines in Figure 4. The reduction of the E-modulus per strain is higher for higher densities. In other words, the difference between the initial stiffness and stiffnesses at higher loading conditions is larger with increasing densities.

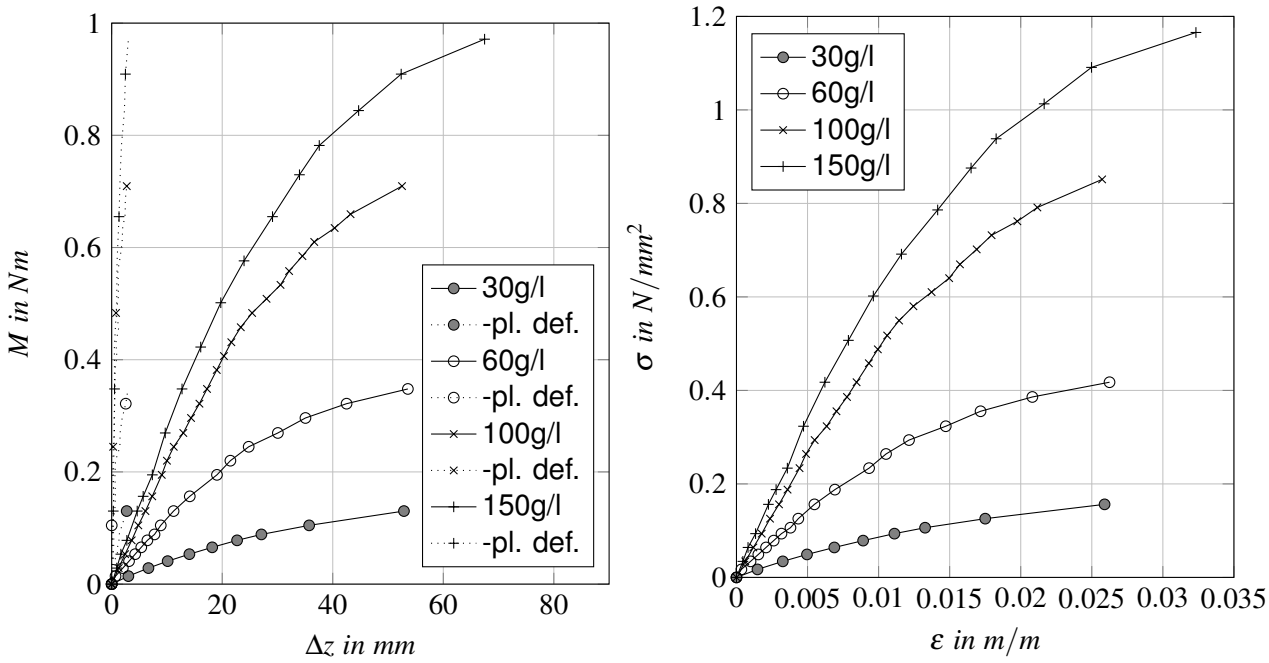

Figure 3 – Three-point-bending curves for four densities of EPP-material

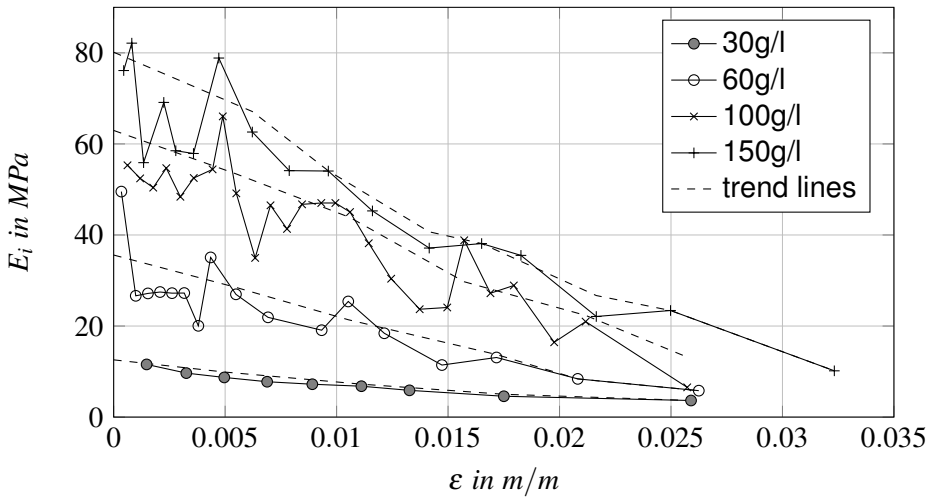

Figure 4 – The obtained E modulus of the multi-linear sections for four densities of EPP-material

4.2 Results of the wind tunnel test

The wind tunnel experiments are carried out with a velocity of 20 m/s. Figure 5 a) illustrates the wing deflection for five angles of attack. The maximum deflection of the wing is shown in Figure 5 b). Just for this image, the velocity was raised up to 50 m/s. The wing did not break and the plastic deformation after a recovery time was very low.

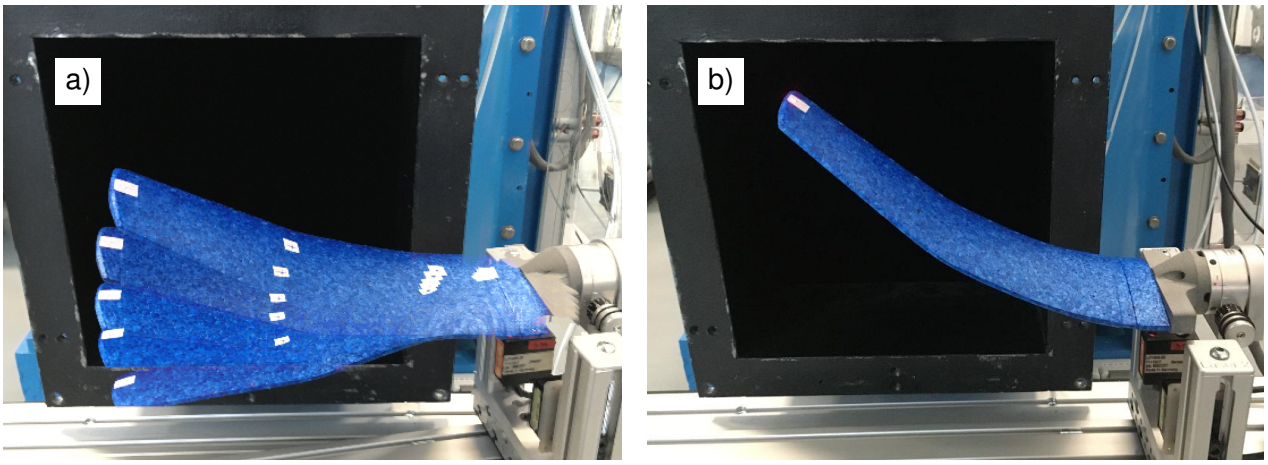

Figure 5 – a) Deflection of the 10°-swept wing for α = -10°, -5°, 0°, 5° and 10° at 20 m/s
b) Maximum deflection of the unswept wing with an angle of attack of 2° at 50 m/s

On the left of Figure 6 and in Figure 7, the deflection of the wingtip (L1) and the half wing span (L2) are depicted over the root bending moment for the three sweep angles (0°, 10° and 20°). The root bending moment is changed by an angle of attack variation. For the low deflection, low load results, a linear regression (dashed lines) is used and extrapolated to show the difference between the initial linear stiffness and the softening effect of the wing. The results of the unswept wing are compared to numerical results which are calculated by the nonlinear elastic beam method and which are shown on the right of Figure 6. The linear results (dotted lines) of the numerical analysis are also calculated with the nonlinear beam method but with a linear material definition which has the same stiffness as the initial stiffness of the nonlinear material definition.

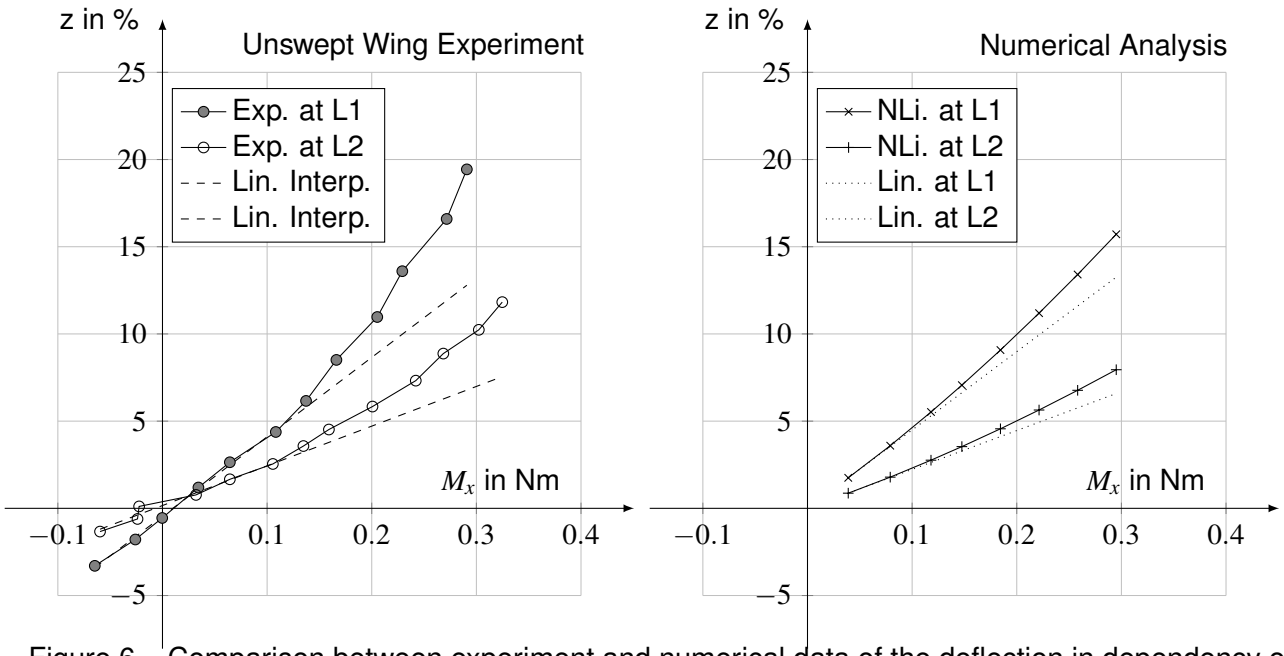

Figure 6 – Comparison between experiment and numerical data of the deflection in dependency of the root bending moment of the unswept 30 g/l-EPP wing

The general trends of the curves in Figure 6 show a good agreement. Both, experimental data and the numerical nonlinear-material data, move apart from their linear results. However, the numerical analysis exhibits a lower gap between nonlinear and linear results than the experimental comparison. This difference indicates that the material of the wing eases more than the material of the flexural test. Furthermore, the geometric data for the numerical results are adjusted as well as possible to the predefined wing structure. In doing so, the dihedral of the outer wing section is neglected in the numerical analysis. So, it is more a qualitative comparison then an exact validation.
The results for the swept wings demonstrate the same softening effect of the foam material. In this campaign also the downward bending of the wing is investigated (see Fig. 7). The softening effect is present on both sides of the wing deflection.

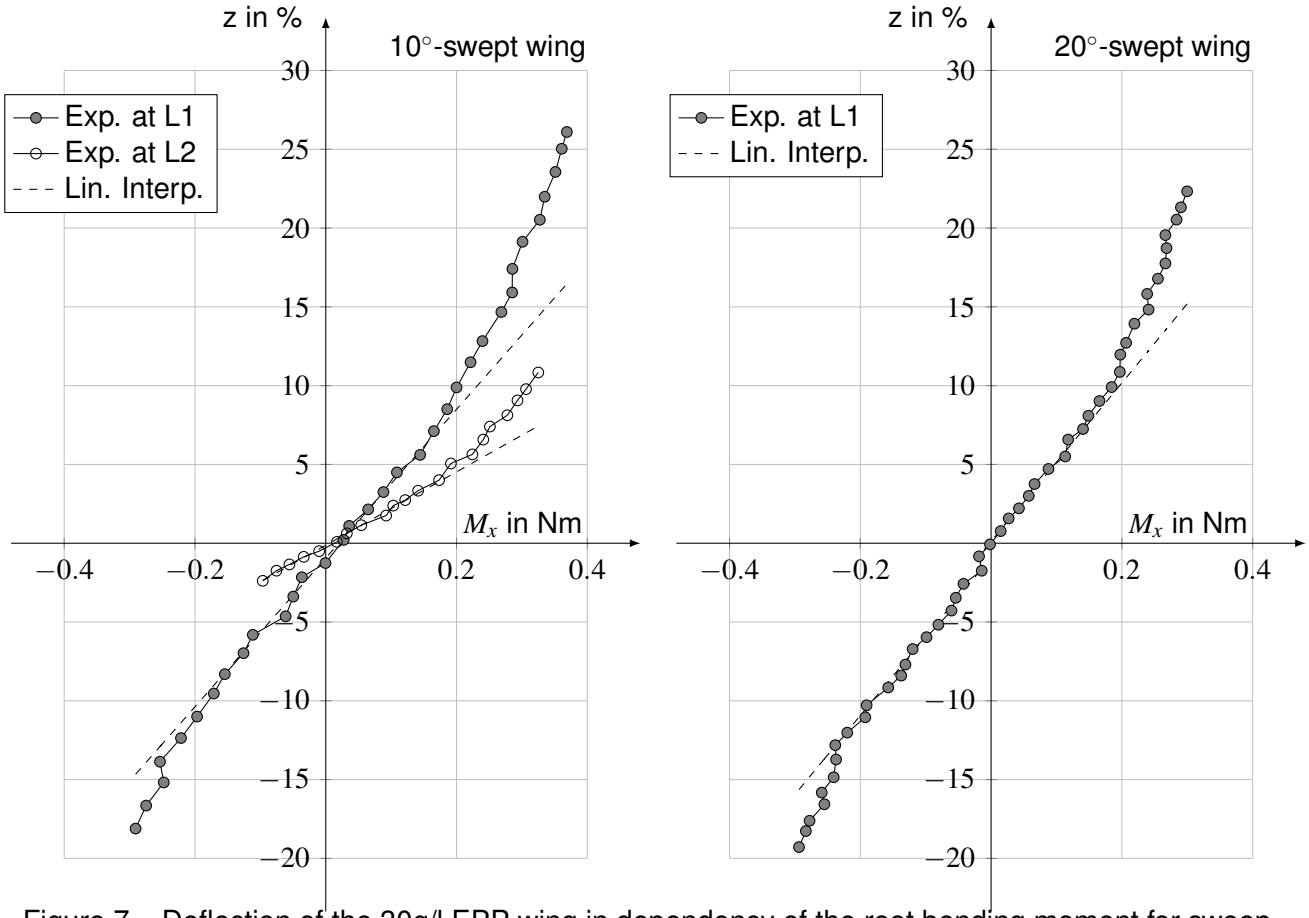

Figure 7 – Deflection of the 30g/l EPP wing in dependency of the root bending moment for sweep angles of 10°and 20°

If the given wing structure and the given material data is now taken for a numerical investigation of an aircraft with this 20°-swept wing, the wing still deflects more than its linear equivalent. In Figure 8 the numerical results are compared with the experiment.
For further investigations, the twist distribution of the nonlinear wing is pretwisted to match the lift distribution of the 1.0 g manoeuvre of the linear variant. Which should be considered as the optimal lift distribution for drag reduction during cruise flight. Due to the more flexible wing for higher loading and the bending-torsion coupling, the lift distribution for a 2.5 g manoeuvre moves inboards, which reduces the root bending moment. The reduction of the root bending moment between the linear and the nonlinear variant is -0.7%.
In conclusion, the softening effect of the nonlinear wing (blue) in contrast to its linear variant (black) is described with the following steps:

- The wing bends up more intensely (Fig. 9 a).
- The incident angle of the outer wing decreases (Fig. 9 b).
- The required lift has to be produced closer to the fuselage (Fig. 9 c).
- The root bending moment is reduced (Fig. 9 d).

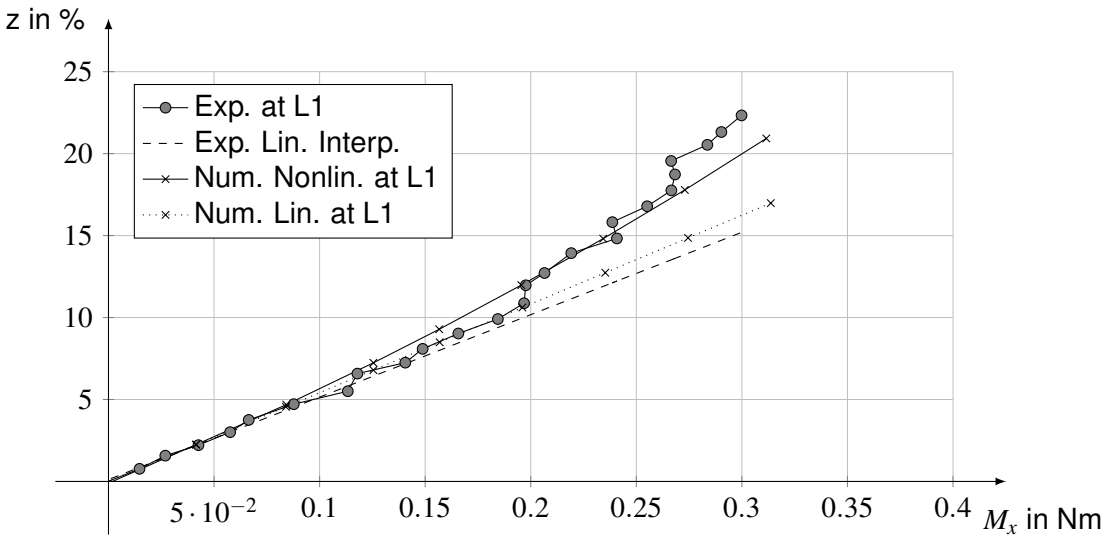

Figure 8 – Comparison between experiment and numerical data of the deflection in dependency of the root bending moment of the 20°-swept wing

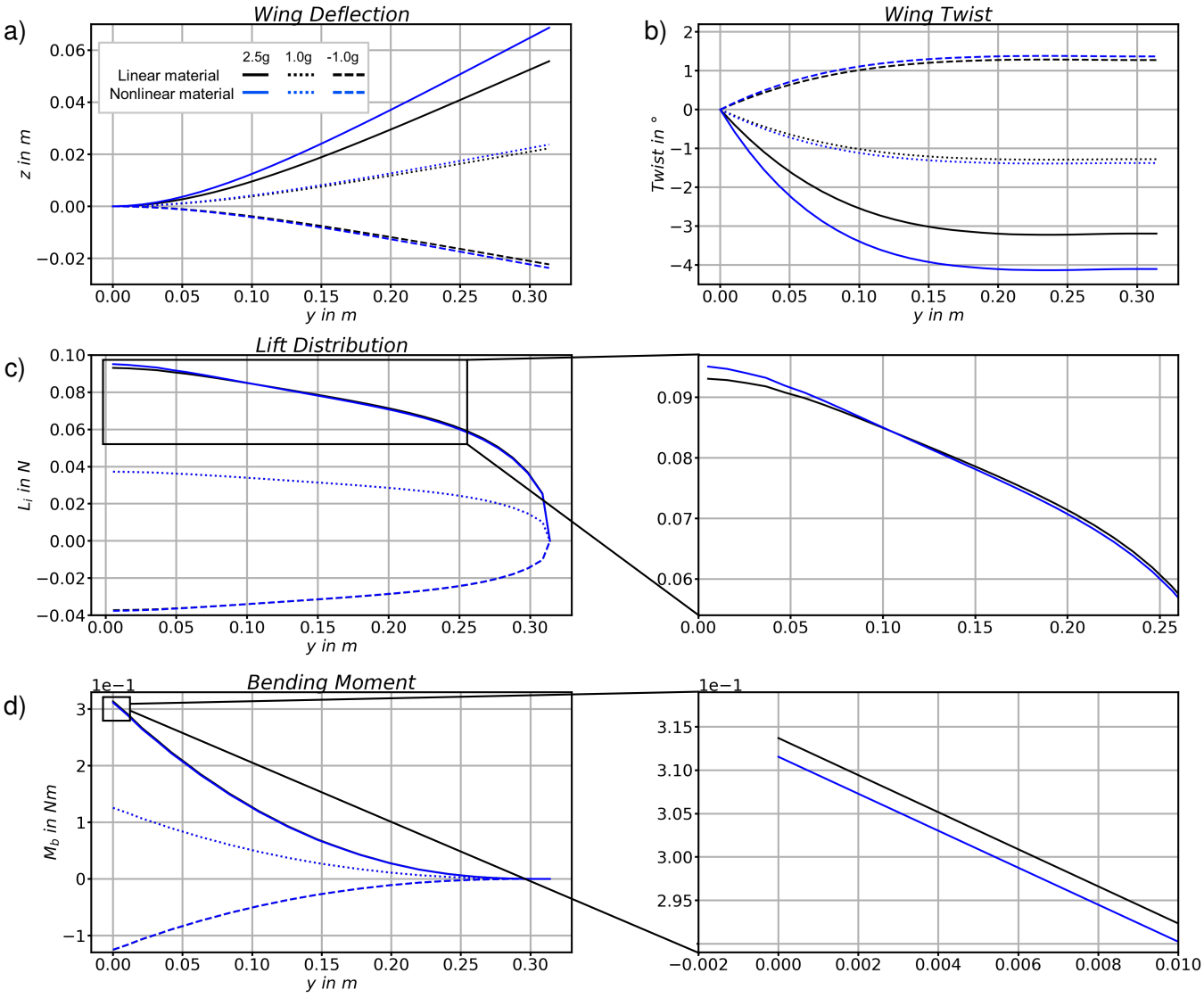

Figure 9 – a) Deflection of the 20°-swept wing for -1.0 g, 1.0 g and 2.5 g manoeuvre, b) Twist distribution, c) Lift distribution, d) Bending moment distribution

5. Conclusion and Outlook

The flexural bending tests characterise the degressive bending stiffnesses of EPP-foam for four densities. It should be pointed out that the degressive stiffness is a combined result of nonlinear elasticity, creeping and plasticity. However, for the realisation of a softening effect at a wing structure, the shares of the three parts in the stiffness composition is not important at this stage. As a consequence, the material represents the properties of a softening structure technology for wings the size of a wind tunnel model.

The EPP-foam wing becomes softer for higher loading conditions which introduces a new way of load alleviation. This can be used for enhancing the 'off'-design cruise flights, while reducing the wing loading of sizing loadcases. For higher reduction of the root bending moment, the softening effect should become active above the cruise flight point. This is not the case with this EPP-foam material. Our previous results [9] predict root bending moment reductions of about 4% if the stiffness reduction becomes active above cruise deflection.

Furthermore, the aeroelastic method for nonlinear elastic beams is capable to analyse multi-linear stiffnesses of wing structures. The missing aspects of this method are the effects of geometrical nonlinearities which become active for deflections above 10%. However, in methods with nonlinear geometrical results of wings with linear stiffnesses (see [10]), the tip deflection is also linear dependent on the root bending moment.

In future, a wind tunnel model for exact validation of the method without dihedral angles and with a higher density is planned. This should be compared with an equivalent wing tunnel model with the initial stiffness of the nonlinear material as linear stiffness. Another idea for a nonlinear elastic wing structure is the use of buckling areas. Here, an investigation on the influence of the softening effect of buckling panels towards the loads is envisaged. Besides, we will analyse a wing tip device with variable stiffnesses which may increase the load alleviation effects of degressive wing structures.

Finally, it can be said that nonlinear elastic stiffnesses are able to reduce loads and a first technology for degressive wing structures has been shown.

Acknowledgments

We would like to acknowledge the funding by the Deutsche Forschungsgemeinschaft (DFG, German Research Foundation) under Germany's Excellence Strategy **EXC 2163/1** - Sustainable and Energy Efficient Aviation (SE^2A) - **Project ID 390881007**.

Copyright Statement

References

[1] Dillinger, J., Static Aeroelastic Optimization of Composite Wings with Variable Stiffness Laminates, Dissertation, TU Delft, Göttingen, 2015.

[2] Stodieck, O., Aeroelastic Tailoring of Tow-Steered Composite Wings, Dissertation, University of Bristol, 2016. doi: 10.13140/RG.2.2.29020.82562

[3] Wilson, T., Kirk, J., Hobday, J., Castrichini, A., Small scale flying demonstration of semi aeroelastic hinged wing tips, International Forum on Aeroelasticity and Structural Dynamics (IFASD), Savannah, Georgia, USA, June 2019.

[4] Gottstein, G., Materialwissenschaft und Werkstofftechnik - Physikalische Grundlagen, Springer Vieweg, Berlin and Heidelberg, 2014.

[5] Münch, M., Rohde, S., Schlimmer, M., Mehrachsige Beanspruchung von thermoplastischen Konstruktionsschaumstoffen, University Kassel, 2002.

[6] Yao, C., Hu, Z., Mo, F., Three-Point Bending Fatigue Behavior of Aluminum Foam Sandwich Panels with Different Density Core Material, Metals, Vol. 11, 2011. https://www.mdpi.com/2075-4701/11/10/1542 doi: 10.3390/met11101542

[7] Weingart, N., Raps, D., Kuhnigk, J., Klein, A., Altstädt, V., Expanded Polycarbonate (EPS) - A New Generation of High-Temperature Engineering Bead Foams Polymers, Vol.12, 2020. https://www.mdpi.com/2073-4360/12/10/2314 doi: 10.3390/polym12102314

[8] Bramsiepe, K., Gröhlich, M., Dähne, S., Hahn, D., Structural Concepts for Passive Load Alleviation, AIAA SCITECH 2022 Forum, San Diego, CA and Virtual, January, 2022. doi: 10.2514/6.2022-0687

[9] Bramsiepe, K., Klimmek, T., Krüger, W., Tichy, L., Aeroelastic method to investigate nonlinear elastic wing structures, CEAS Aeronautical Journal, 2022

[10] Ritter, M., Cesnik, C., Large Deformation Modeling of a Beam Type Structure and a 3D Wingbox using an Enhanced Modal Approach, 57th AIAA/ASCE/AHS/ASC Structures, Structural Dynamics, and Materials Conference, at the AIAA SciTech 2016 Forum, San Diego, CA, 2016. https://elib.dlr.de/102741/